J Mol Model (2001) 7:20–25
DOI 10.1007/s008940100010

ORIGINAL PAPER

**Kuo-Long Lou · Hsiu-Chuan Chou · Yau-Wei Tsai
Yu-Shuan Shiau · Po-Tsang Huang · Ting-Yu Chen
Yuh-Yuan Shiau · Robert J. French**

Involvement of a novel C-terminal kinase domain of Kir6.2 in the K-ATP channel rundown reactivation

Received: 24 October 2000 / Accepted: 1 February 2001 / Published online: 4 April 2001

Abstract Rundown is a generally encountered problem while recording K_{ATP} channel activity with inside-out patches. No assigned structural fragment related to this mechanism has yet been derived from any of the functional analyses performed. Therefore, based on a combined sequence and secondary structure alignment against known crystal structure of segments from closely related proteins, we propose here the three-dimensional structural model of an intracellular C-terminal domain of the Kir6.2 subunit in K_{ATP} channels. An *E. coli* CMP-kinase was suggested as template for the model building. The subdomain arrangement of this novel kinase domain and the structural correlation for UDP-docking are described. With structural-functional interpretation, we conclude that the reactivation of K_{ATP} channel rundown by MgATP or UDP is very possibly regulated by this intracellular kinase domain at the C-terminus of Kir6.2 subunit in K_{ATP} channels.

Keywords Channel gating · 3D homology modeling · Kinase domain · Kir6.2 · Rundown reactivation

Introduction

ATP-sensitive K^+-channels (K_{ATP} channels or K-ATP channels) are distributed in a wide variety of tissues, including brain nerve cells, cardiac and skeletal muscles, and pancreatic β-cells [1, 2, 3]. They play a pivotal role in coupling membrane excitation to cellular metabolism. The molecular architecture of K_{ATP} channels is an octameric complex of two structurally unrelated subunits that assemble with 4: 4 stoichiometry [4, 5, 6]. The ion-pore subunits are members of the inwardly rectifying potassium channel family (Kir), which have two membrane-spanning domains (M1 and M2) flanking the K^+-selective ion-pore region (H5) and cytoplasmic amino (N-) and carboxyl (C-) termini [7]. The regulatory subunits are sulfonylurea receptors (SUR), members of the ATP-binding cassette superfamily which have two intracellular nucleotide binding folds, NBF1 and NBF2 [8].

The regulation of K_{ATP} channel activity by cytosolic constituents is extremely complex and is still not fully understood. In addition to the ATP-dependent channel closure under physiological conditions, some cytosolic agents are required to maintain the ability of the channel to enter the open state, because after formation of an inside-out patch the activity of the channel declines with time. This phenomenon has been described as rundown for K_{ATP} channels [9, 10, 11, 12, 13]. Providing that channel activity has not completely vanished, it can be partially restored by brief exposure of the patch to MgATP or UDP [10, 11, 12, 13, 14, 15, 16, 17]. It has been proposed that this reactivation might involve protein phosphorylation on residues other than serine/threonine in Kir6.2 and that the hydrolysis energy of MgATP seems to be utilized for such reactivation [9, 10, 18, 19, 20]. However, the ability of MgATP to reactivate the channel activity is variable, declines with time and is ineffective after complete rundown; it is, therefore, also suggested that an endogenous kinase responsible for phosphorylation might exist and is gradually inactivated or lost from the patch membrane with time [11]. Moreover, trypsin digestion of Kir6.2 leads to the prevention of rundown, indicating an exposed binding fold responsible for the deduced conformational change and the rundown mechanism [11, 21]. On the other hand, UDP can also reactivate the K_{ATP} channel rundown, which is pre-

K.-L. Lou (✉) · H.-C. Chou · Y.-W. Tsai · P.-T. Huang
T.-Y. Chen · Y.-Y. Shiau
Graduate Institute of Oral Biology, College of Medicine,
National Taiwan University, Taipei 10042, Taiwan
e-mail: kllou@ha.mc.ntu.edu.tw
Tel.: +886 2 23562340, Fax: +886 2 23820785

Yu-Shuan Shiau
Institute of Statistical Science, Academia Sinica, Taipei, Taiwan

Robert J. French
Department of Biophysics & Neuroscience Research Groups,
Faculty of Medicine, Health Sciences Centre,
University of Calgary, T2N 4N1, Canada

sented in different kinetic styles between Kir6.1 and Kir6.2 [13]. Whether a common structural motif or a similar pathway and/or mechanism is involved in the reactivation by MgATP and UDP remains controversial [13]. Currently, however, no direct structural evidence is available to indicate the reactivation mechanism of K_{ATP} channel rundown. Therefore, based on a combined sequence and secondary structure alignment against known crystal structure of segments from closely related proteins, we propose here a three-dimensional (3D) structural model of the intracellular part of the Kir6.2 subunit of K_{ATP} channels. A kinase domain was suggested for the C-terminal residue region. For further investigation of the molecular catalytic behavior of this kinase domain, nucleotide-docking simulation was accomplished. The residues required for binding contacts with nucleotides in our structural model are also described in this paper.

Methods

Search for templates. The BLAST algorithm was employed to search in PDB for protein segments whose sequences are similar to that of mouse Kir6.2 (Genbank accession number S68403) and whose structures can serve as viable structural templates. The crystal structures of *E coli* CMP-kinase (CKE, 6137462) (free and in complexed forms) [22, 23] were chosen for the determination of structurally conserved regions (SCRs). The Kir6.2 residues used for model building are according to their paired sequence (see below) compared to the CKE sequence. In addition, immediately after the primary sequence comparison with BLAST, residues before 228 were eliminated according to the results.

Paired sequence alignment. The GCG program was used to determine the equivalent residues. Residue regions of CKE represented as continuous lines dominantly observed were employed as appropriate template regions and the corresponding fragments in Kir6.2 were chosen for alignment. The amino acid sequences of these Kir6.2 fragments were then included in the multiple sequence alignment of the appropriate CKE regions to specify the residue numbers for model building [24].

Model building and docking simulation for nucleotides. Modeling by homology was performed essentially by following the procedures described by Siezen [24]. Briefly, the residue fragments of Kir6.2 were chosen according to the results from GCG paired sequence alignment. They were then superimposed on to the crystal coordinates of the Cα atoms of the corresponding SCRs from the CKE structure. This generated the secondary structure and relative position of the definite secondary structural elements in the chosen residue fragments of Kir6.2. Junctions between the secondary structural elements were individually regularized by energy minimization to give reasonable geometries.

The UDP and CDP molecules were created from small molecule units in a databank via modification with the cvff force field. Upon docking, the total energy and van der Waals' contacts between the complexes of CDP- and UDP-binding to Kir6.2 model were compared. Distribution of surface charges via electrostatic potentials was performed by exhibiting the Connolly surfaces for the binding residues from the kinase domain on Kir6.2.

All the calculations and structure manipulations described above were performed with the Discover/Insight II molecular simulation and modeling program (Molecular Simulation, San Diego, CA, USA; 950 release) on a Silicon Graphics Octane/SSE workstation.

Fig. 1 Sequence alignment of Kir6.2 and CKE. The residues of Kir6.2 (Genbank accession number S68403) identical to those of template *E coli* CMP-kinase (CKE, 6137462) are in red, whereas the conservative substitutions are in green. Two corresponding residue fragments chosen according to the results of paired sequence alignment are compared. The residue identity for each fragment: (*upper part*) 33.96% for residues 229 to 281; (*lower part*) 27.08% for residues 338 to 385 (rmsd=0.349 and 0.354, respectively). All amino acid residues are represented with single-letter abbreviation

Results and discussion

Paired sequence and structural alignment

From the BLAST results, the crystal structures of *E coli* CMP-kinase (CKE, 6137462) (free and in complexed forms) [22, 23] were chosen as template protein and for the determination of structural conserved regions (SCRs). Sequence comparison and the residue identities between Kir6.2 and CKE are shown in Fig. 1. Two residue fragments of Kir6.2 were chosen according to the results from GCG paired sequence alignment, and then used for structural alignment. These are residues 229–281 and 338–385 (from N- to C-termini of Kir6.2), for which residues 3–54 and 62–113, respectively, of CKE are applied to create coordinates (Figs 1 and 2). This modeled part of the molecule is located on the intracellular C-terminus of Kir6.2.

Overall structural features and comparison with the template

Structural information from our model suggests a novel kinase domain at the intracellular C-terminus of the Kir6.2 subunit with the subdomain arrangement that is very similar to those observed in the crystal structure of *E. coli* CMP-kinase (CKE) and of other NMP kinases [22, 23]. Fig. 2 shows a comparison of the folding patterns of CKE and this novel kinase domain of Kir6.2 C-terminus. A binding cleft for nucleotides can be observed in the upper middle part of the structure in both molecules (Fig. 2).

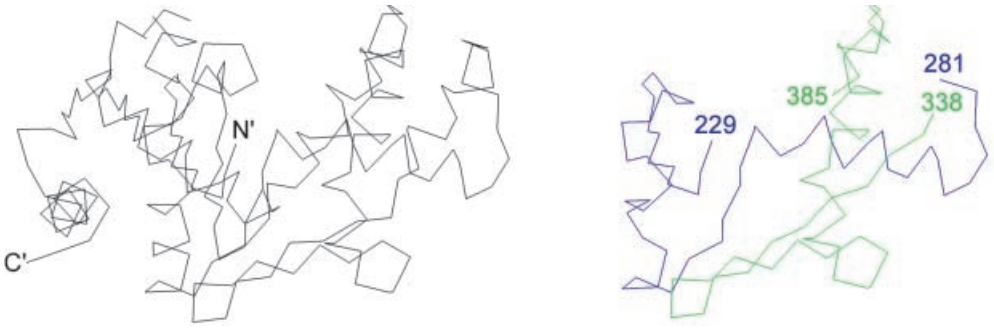

Fig. 2 Comparison of Cα-tracing between CKE crystal structure (*left*) and the structural model of Kir6.2 intracellular kinase domain (*right*). The residue numbers indicated in the kinase domain structure are to distinguish the connections for the two separate residue fragments. Both diagrams are viewed with the binding cleft facing upside. Drawings in all the figures (Fig. 2, Fig. 3, Fig. 4, Fig. 5) were made with Insight II software package

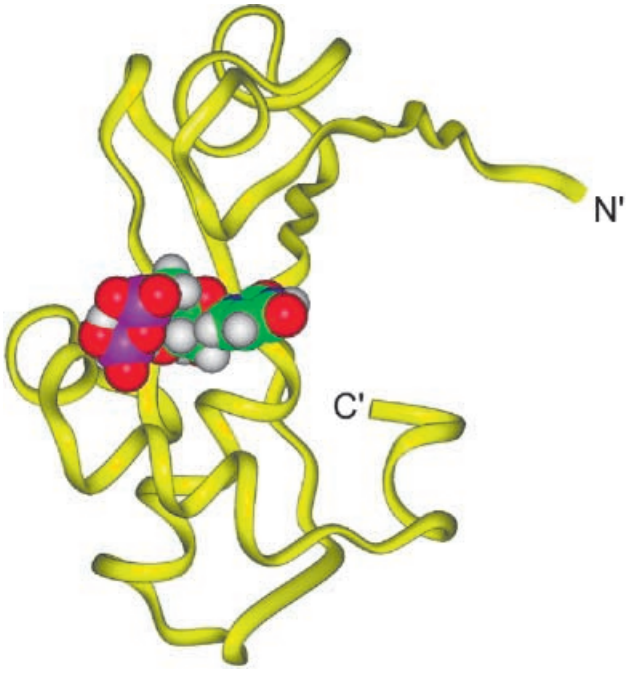

Fig. 3 3-D structural model of the intracellular kinase domain of Kir6.2 in docking with the UDP molecule. The kinase domain is drawn as yellow ribbons and the N- and C-termini are indicated. The UDP molecule is drawn with CPK spheres in different colors according to the type of atoms. Viewing is directly towards the binding cleft

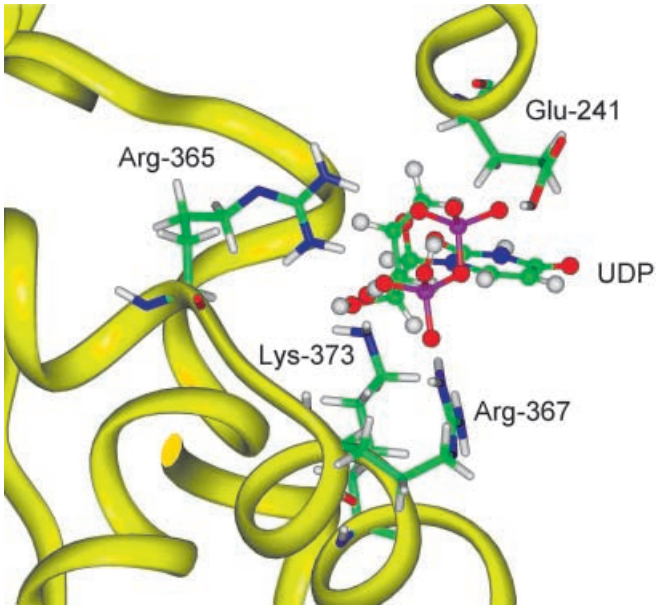

Fig. 4 Close view of the binding cleft with the UDP molecule. The Kir6.2 kinase domain is drawn as the yellow ribbon, whereas UDP molecule is depicted as ball-and-stick models in various colors according to the atom types. Side-chains of the Kir6.2 residues that might interact or form putative hydrogen bonds with the UDP molecule are shown as sticks in colors according to the types of atoms, with residue number indicated

Nucleotide binding

For further investigation of the molecular catalytic behavior of this kinase domain, or, to confirm the role this novel deduced kinase domain may play in Kir6.2, the nucleotide-docking simulation was accomplished. Energy minimization gave a very stable conformation for both UDP and CDP molecules upon binding to this kinase domain (CDP-form/UDP-form: –625.77/–621.45 (kcal mol^{-1}) for total energy; 253.42/253.28 for van der Waals' contact; rmsd=0.110/0.103). Fig. 3 illustrates the binding of UDP with our structural model. The UDP molecule is located and properly oriented in the binding cleft flanked by several α-helices of which the residue side-chains protrude towards UDP to form binding contacts. The details of the side-chain contacts are shown in Fig. 4.

Because such structural models do not give sufficient detail to enable us to measure the hydrogen-bonding distances, we can merely depict here what we have observed from the structure in Fig. 4 regarding the interaction between the corresponding atoms from residue side-chains of Kir6.2 and from the UDP molecule. These residues of Kir6.2 are: Arg-365, Arg-367, Lys-373 on one side of UDP and Glu-241 on the other side. They form putative hydrogen-bonds between UDP and Kir6.2 in the appropriate orientation and in a reasonable range of spa-

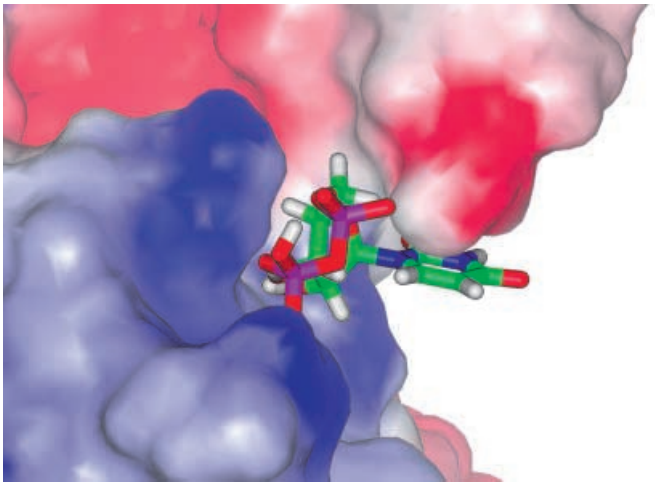

Fig. 5 Electrostatic potential surfaces for the UDP-binding pocket of Kir6.2. Red corresponds to an electrostatic potential of ≤–5 k_BT/e, white an electrostatic potential 0 k_BT/e and blue an electrostatic potential of ≥+5 k_BT/e. The UDP molecule is drawn as sticks in color according to the types of atoms. The orientation of molecules is almost the same as observed in Fig. 4.

tial distance. This might imply and emphasize the utilization of UDP by this kinase domain on Kir6.2.

To describe further the binding ability and the residue contacts, the electrostatic potential surfaces for the binding pocket on Kir6.2 are depicted in Fig. 5. This confirms again the appropriate and reasonable binding contacts between the Kir6.2 cleft and UDP upon docking.

It is interesting to note that:

1. the two parts of Kir6.2 residues forming H-bonds with UDP come from the two separate residue fragments mentioned previously in the structural alignment section; and
2. they are all charged residues.

Such facts or observations indicate that they are indeed appropriate to contribute to the construction of the binding moiety and form H-bonds with nucleotides upon docking. Such information might, therefore, enable us to make decisions on selecting reasonable candidates for site-directed mutagenesis and then further to verify the role of this kinase domain in the reactivation of K_{ATP} channel rundown for investigation in the future.

Structural–functional interpretation

The most important structural-functional interpretation provided by this 3-D structural model is with respect to the reactivation of K_{ATP} channel rundown. As has been described in the introduction, providing the channel activity has not completely vanished, it can be partially restored by brief exposure of the patch to MgATP and UDP [10, 11, 13, 19]. Such reactivation might involve protein phosphorylation on residues other than serine/threonine in Kir6.2 and the hydrolysis energy of MgATP seems to be utilized. In addition, the ability of MgATP to reactivate the channel activity declines with time and is ineffective after complete rundown. All this suggested that an endogenous kinase responsible for subsequent phosphorylation should exist and is gradually inactivated or lost from the patch membrane with time [11].

One explanation of these results is that the K_{ATP} channel complex can exist in an active, phosphorylated state and an inactivated, dephosphorylated state. Dephosphorylation by membrane-associated phosphatases causes the channel to enter a closed (or, here, inactivated) state from which it can only exit on phosphorylation by an endogenous kinase. Thus in the absence of MgATP, channel activity will slowly run down as more channels enter the dephosphorylated closed state.

We propose that such phosphorylation should occur via this novel kinase domain at the C-terminus of Kir6.2. The following statements might clarify and support such a hypothesis. One should not forget that the rundown of K_{ATP} channels can be also reactivated by exposure of the patch to UDP. This kinase domain provides an obvious link between the MgATP- and UDP-reactivation of channel rundown. The template protein, CMP-kinase, was proposed to be CMP-specific in prokaryotes and CMP/UMP-dispensable in eukaryotes [22]. If we look into the reversible reaction of this kinase, a spectrum of agents required for channel gating could be observed. This kinase uses MgATP to produce UDP and MgADP when UMP is present. Vice versa, when UDP is applied, MgADP can be used to generate MgATP. This explains at least in part why MgATP and UDP can both reactivate the channel rundown, and, as a consequence, describes the utilization of the hydrolysis energy of MgATP for channel phosphorylation through an endogenous pathway. Some aspects still should be clarified, however. For example:

1. the exact phosphorylation site(s) which can allow channels to enter the activatable state via MgATP hydrolysis and subsequent phosphorylation; and
2. the involvement of other membrane-associated or non-associated components contributing to phosphorylation/dephosphorylation, e.g. PIP_2, Ca^{2+} and PKC, instead of this kinase domain alone, in the rundown and in its reactivation.

The second aspect will bring the emphasis to the mutual interactions among those components, i.e., the signaling pathway and the mechanism evoking the slow-phase rundown via Kir6.2 [25]. In addition, it is also very important to identify the structural requirement that serves as the rest part of the nucleotide-binding moiety. Regarding this part, the N-terminal residues of Kir6.2 seem to satisfy such purpose upon considering the tetrameric assembling structural characteristics of

these K-channel family members [26, 27], and, therefore, an interaction involving both N- and C-termini of Kir6.2 with respect to the complexity of gating can be expected.

Recently, studies by several groups [17, 25] have successfully demonstrated that both fast-phase (short-term) and slow-phase (long-term) types of rundown may exist. The former is induced by interaction with SUR subunit and can be recovered by the regulation of MgADP/MgATP [28]. The latter is supposed to result from either subunit uncoupling [29, 30] or direct dephosphorylation on Kir6.2 via, for instance, Ca^{2+}, and can be reactivated by addition of PIP_2 and MgATP through pathways involving kinases [25, 31]. Before the patch excision or channel rundown, the K_{ATP} channel activity can be maintained by the regulation of SUR via subunit coupling [25, 29] or the deletion of 26 C-terminal residues [30] in the absence of physiological concentrations of ATP, which binds to the channels to induce the inhibition. Meanwhile, the phosphorylation on Kir6.2 by endogenous kinases maintains the channels in the activatable state. Excision of the patch results in the time-dependent loss of endogenous membrane-associated kinases and the activatable state for channels cannot be maintained. The channels become gradually dephosphorylated by phosphatases. Once K-ATP channels enter the long-term rundown phase, such dephosphorylated, inactivated state of Kir6.2 can be reactivated only by those pathways inducing kinase phosphorylation, for instance, the addition of specific/non-specific kinases in patch solution, upon utilization of MgATP, then back to phosphorylated and activatable state [25]. It is, therefore, quite obvious that MgATP has its own dual effects, either inhibits through SUR regulation or direct binding on Kir6.2, or reactivates the channels in the rundown events. In addition, the direct binding of MgATP to Kir6.2 can be prevented by PKC through electrostatic effect (unpublished data). However, the existence of a kinase domain at Kir6.2 C-terminus, in all cases, confirms the possibility for and provides an alternative for or assists the utilization of ATP. Furthermore, our results supplemented the information required to explain the findings by Noma's group [17] in which the long-term rundown phase can be recovered more efficiently in the presence of UDP. All this provides indeed a very fresh insight into the K_{ATP} channel rundown phenomenon. However, whether it is economic for Kir6.2 to include an intrinsic kinase domain, instead of using another coupling molecule, remains to be clarified.

Conclusion

Our model has for the first time described three-dimensional structural information for subdomain arrangement of the residues at the intracellular C-terminus of Kir6.2 and the structural correlation for nucleotide-binding, as well as the functional implication of such a putative kinase domain. Because of the limitation of predictive structural model, only the structural correlation derived from the reported functional results related to rundown reactivation was discussed in this paper. Nevertheless, such information provides directions for further functional assays and choices of the appropriate candidate for site-directed mutagenesis before the crystal structure of Kir6.2 is determined.

Acknowledgements The authors would like to thank Ting-Lin Chien and Yi-Chun Tsai at Hitron Technology for their technical advice. We are also very grateful to Drs W. F. van Gunsteren and Daniela Pietrobon for their advisory discussion and helpful suggestions. This work was supported in part by Research Grants from NTUMC R&D Committee: 89-N4;CNB 88–03 (88.1.1.-88.12.31.) and 89D118 (89.4–8), and from National Sciences Council of Taiwan: NSC 89–2314-B-002–258 (1999.8.1–2000.7.31) and 89–2320-B-002–234 (2000.8.1.-2001.7.31.) for L.K.L.

References

1. Ashcroft, F. M.; Ashcroft, S. J. H. *Cell. Signal.* **1990**, *2*, 197–214.
2. Ashcroft, F. M.; Gribble, F. M. *TINS* **1998**, *21*, 288–294.
3. Inagaki, N.; Tsuura, Y.; Namba, N.; Masuda, K.; Gonoi, T.; Horie, M.; Seino, Y.; Mizuta, M.; Seino, S. *J. Biol. Chem.* **1995**, *270*, 5691–5694.
4. Inagaki, N.; Gonoi, T.; Clement, J. P., IV; Namba, N.; Inazawa, J.; Gonzalez, G.; Aguilar-Bryan, L.; Seino, S.; Bryan, J. *Science* **1995**, *270*, 1166–1170.
5. Inagaki, N.; Gonoi, T.; Seino, S. *FEBS Lett*. **1997**, *409*, 232–236.
6. Shyng, S.-L.; Nichols, C. G. *J. Gen. Physiol*. **1997**, *110*, 655–664.
7. Isomoto, S.; Kondo, C.; Kurachi, Y. *Japan. J. Physiol.* **1997**, *47*, 11–39.
8. Aguilar-Bryan, L.; Nichols, C. G.; Wechsler, S. W.; Clement, J. P., IV; Boyd, A. E., III; González, G.; Herrera-Sosa, H.; Nguy, K.; Bryan, J.; Nelson, D. A. *Science* **1995**, *268*, 423–426.
9. Findlay, I. *Pflüg. Arch.* **1987**, *410*, 313–320.
10. Ohno-Shosaku, T.; Zünkler, B. J.; Trube, G. *Pflüg. Arch.* **1987**, *408*, 133–138.
11. Proks, P.; Ashcroft, F. M. *Pflüg. Arch.*, **1993**, *424*, 63–72.
12. Takano, M.; Qin, D.; Noma, A. *Am. J. Physiol.* **1990**, *258*, H45–50.
13. Takano, M.; Xie, L.-H.; Otani, H.; Horie, M. *J. Physiol. (London)* **1998**, *512.1*, 395–406.
14. Findlay, I.; Dunne, M. J. *Pflüg. Arch.* **1986**, *407*, 238–240.
15. Misler, S.; Falke, L. C.; Gillis, K.; McDaniel, M. L. *PNAS USA* **1986**, *83*, 7119–7123.
16. Trube, G.; Hescheler, J. *Pflüg. Arch.* **1984**, *401*, 178–184.
17. Xie, L.-H.; Takano, M.; Kakei, M.; Okamura, M.; Noma, A. *J. Physiol. (London)* **1999**, *514*, 655–665.
18. Findlay, I. *J. Physiol. (London)* **1987**, *391*, 611–631.
19. Furukawa, T.; László, V.; Furukawa, N.; Sawanobori, T.; Hiraoka, M. *J. Physiol. (London)* **1994**, *479.1*, 95–107.
20. Kozlowski, R. Z.; Ashcroft, M. L. J. *Proc. R. Soc. Lond. [biol]* **1990**, *240*, 397–410.
21. Proks, P.; Ashcroft, F. M. *J. Physiol. (London)* **1993**, *459*, 240P.
22. Briozzo, P.; Golinelli-Pimpaneau, B.; Gilles, A. M.; Gaucher, J. F.; Burlacu-Miron, S.; Sakamoto, H.; Janin, J.; Barzu, O. *Structure* **1998**, *6*, 1517–1527.
23. Bucurenci, N.; Sakamoto, H.; Briozzo, P.; Palibroda, N.; Serina, L.; Sarfati, R. S.; Labesse, G.; Briand, G.; Danchin, A.; Barzu, O.; Gilles, A. M. *J. Biol. Chem.* **1996**, *271*, 2856–2862.

24. Siezen, R. J.; Rollema, H. S.; Kuipers, O. P.; de Vos, W. M. *Prot. Engineer.* **1995**, *8*, 117–125.
25. Ribalet, B.; John, S. A.; Weiss, J. N. *J. Gen. Physiol.* **2000**, *116*, 391–409.
26. Morais-Cabral, J. H.; Lee, A.; Cohen, S. L.; Chait, B. T.; Li, M.; Mackinnon, R. *Cell* **1998**, *95*, 649–55.
27. Proks, P.; Gribble, F. M.; Adhikari, R.; Tucker, S. J.; Ashcroft, F. M. *J. Physiol. (London)* **1999**, *514*,19–25.
28. Gribble, F. M.; Tucker, S. J.; Ashcroft, F. M. *EMBO J.* **1997**, *16*, 1145–1152.
29. Koster, J. C.; Sha, Q.; Nichols, C. G. *J. Gen. Physiol.* **1999**, *114*, 203–213.
30. Tucker, S. J.; Gribble, F. M.; Zhao, C.; Trapp, S.; Ashcroft, F. M. *Nature* **1997**, *387*, 179–182.
31. Ribalet, B.; Ciani, S.; Eddlestone, G. T. *J. Gen. Physiol.* **1989**, *94*, 693-717.